Examinations of viscous dissipation, magnetic field and thermal radiation on the systematic flow of Casson fluid with gyrotactic microorganisms

Abubakar Usman[1*]

[1]Department of Mathematics and Statistics, Hassan Usman Katsina polytechnic, Katsina State, Nigeria.

Abstract. This research work is aimed at examining the significance of viscous dissipation, magnetic field alongside thermal radiation on the flow of Casson fluid. The fluid flow was considered in the presence of gyrotactic microorganisms and nanoparticles. The physics of the problem is governed with partial differential equations (PDEs). The set of PDEs are changed to ordinary differential equations (ODEs) by utilizing an appropriate similarity variables. To examine the pertinent flow parameters, a numerical approach called spectral relaxation method (SRM) was employed. This SRM approach employs the basic Gauss-seidel method to decouple and descritize the set of differential equations. The choice of this approach is due to its consistency and accuracy. The viscous dissipation parameter (Ec) was found to enhance fluid temperature, velocity and boundary layers (thermal and momentum boundary layer). The strong opposition of magnetic parameter give rise to lorenz force which drags the fluid flow within the boundary layer. The nanoparticles was found to bare great effect on the gyrotactic microorganisms.

1 Introduction

In recent years, significant attention has been devoted to understanding the impact of viscous dissipation on unsteady mixed convection, owing to its practical relevance across various fields including medical chemistry, medicine, engineering and industries. The utilization of nanofluids in thermal systems, characterized by the presence of ultrafine solid particles, is steadily increasing. Nanofluids offer promising alternatives as working fluids in energy devices. Numerous studies have investigated the thermophysical properties, heat, and fluid flow characteristics of nanofluids in various systems, aiming to uncover their advantages over conventional working fluids. Thermophoresis, a branch of applied mathematics, deals with the movement of small particles, such as dust, from hot surfaces towards colder ones. This phenomenon finds diverse applications, including the removal of small particles from

*Corresponding author: abubakarusman847@gmail.com

gas streams, tracking the curved paths of particles emitted by combustion devices, and exploring particle deposition on turbine blades.

Aiyashi et al., [1] discovered that the temperature, velocity, volume fraction, Sherwood number, and Nusselt number are significantly influenced by both the magnetic field and viscous dissipation in an unsteady mixed convective stagnation point flow of nonhomogeneous nanofluid. These findings underscore its potential applicability across various domains, including medical engineering, nanotechnology, and petroleum extraction. Hassan et al., [2] focuses on the investigation of two-dimensional magneto-hydrodynamic Casson fluid dynamics, incorporating phenomena such as heat generation, viscous dissipation, chemical reactions, and the impact of thermal radiation. Both (PST) and (PHF) which are prescribed surface temperature and prescribed heat flux scenarios are examined to explore the problem comprehensively. Kodi et al., [3] discovered the effect of heightened Newtonian heating, revealing a gradual decrease in heat transfer degree at the plate. Additionally, they observed a decrease in fluid concentration due to the influence of a chemical reaction. Obalalu, [4] discovered that considering the second-order terms in the boundary conditions significantly impacts fluid flow characteristics while having no effect on heat transfer characteristics. Qasim and Noreen [5] elucidate that dual solutions may exist within a certain series of the suction parameter. In both instances, it is observed that the momentum boundary layer thickness decreases as the Casson fluid parameter increases. Moreover, the thermal boundary layer thickness exhibits a reduction with rising Prandtl numbers, but an augmentation with increasing Eckert numbers across both scenarios. Furthermore, in the first solution, the thermal boundary layer thickness diminishes as the wall mass suction values escalate, whereas in the second solution, it amplifies with higher values of the mass suction parameter.

Usman et al., [6] explored the influence of the Casson parameter, observing its augmentation of velocity contours and the thickness of the hydrodynamic boundary layer. Furthermore, an increase in the magnetic parameter leads to the generation of Lorentz force, consequently impeding the fluid motion. Additionally, the presence of thermal radiation results in elevated temperatures within the boundary layer. Casson fluids find major applications in polymer processing and biomechanics, with examples including jelly, tomato sauce, fruit juices and honey. Several studies have investigated Casson fluid behavior under various external effects, including magneto-hydrodynamics convection, thermal radiation, and viscous dissipation. Viscous dissipation, characterized by the destruction of velocity profiles due to applied viscous stress, is considered a significant phenomenon in fluid mechanics, involving the transformation of kinetic energy into internal energy within the fluid domain. Studies have explored its effects on Casson fluid flow under different conditions, shedding light on phenomena such as free convection, boundary layer flow, Marangoni convective two-phase flow, and entropy generation. These investigations contribute to a deeper understanding of complex fluid dynamics and their practical implications in various engineering and scientific fields.

Malik et al., [7] proposes a novel coefficient within the conjugate gradient method to address unconstrained minimization problems. This coefficient is derived from a modification of the NPRP (2009) coefficient. Their numerical findings indicate that the proposed method exhibits favorable performance in resolving unconstrained minimization problems. Muhammad et al., [8] observed that magnetism attenuated velocity and the hydrodynamic boundary layer owing toward the presence of Lorentz force. They noted that the Deborah number augmented velocity contour. Furthermore, they found that the Eckert number enhanced the temperature profile as a consequence of temperature generation in the boundary layer. An elevation in the Prandtl number was associated with an improvement in both hydrodynamic and thermal boundary layer thickness. Moreover, the elevation of Dufour parameter was found to elevate local skin friction and Nusselt number.

2 Flow governing equations

This paper presents a mathematical model describing the free convective flow of Casson fluid in the presence of viscous dissipation, magnetic fields, thermal radiation, and gyrotactic microorganisms. Utilizing appropriate boundary layer approximation theory, the constitutive relations of Casson fluid yield the governing equations for the flow. The equations governing continuity, conservation of momentum, energy, and concentration are expressed along with pertinent boundary conditions are as follows:

3 Technique procedure

The boundary value problem technique entails transforming highly nonlinear partial differential equations into first-order ordinary differential equations by introducing a new set of variables of our own selection. Similarly, the boundaries undergo transformation based on analogous assumptions. To ensure more accurate results, a minimal convergence criterion or tolerance is established.
Procedure:

i. Convert highly nonlinear partial differential equations into as system of first-order ordinary differential equations via a newly defined set of variables.
ii. Transform the boundaries using similar suppositions.
iii. Establish a minimal convergence criterion to accomplish a higher accuracy in the results.

The movement of Casson nanofluids occurs as a result of the stretching of the inclined surface of the plate, along with the application of a uniform strength magnetic field (B_0) in the y-axis direction. The concentration of the model species is considered sufficiently high, necessitating the consideration of Soret and Dufour effects. A $T_w < T_\infty$ and $C_w < C_\infty$ scenario with a cooled inclined plate is considered. This research looks at a non-Newtonian Casson nanofluid model with two fluid parameters. The concept of viscosity stated by Idowu and Falodun [9] as $\left(\tau = \mu \frac{\partial u}{\partial y}|_y = 0\right)$ is in compliance aligns with the principles laid out by Fredrickson [10], and the description is articulated in accordance with the flow constitutive equations for Casson as:

$$\tau_{ij} = \left(\mu_b(T) + \frac{P_y}{\sqrt{2\pi}}\right) 2e_{ij} \quad when \quad \pi > \pi_c \tag{1}$$
$$\tau_{ij} = \left(\mu_b(T) + \frac{P_y}{\sqrt{2\pi_c}}\right) 2e_{ij} \quad when \quad \pi < \pi_c$$

where P_y is the fluid yield stress and is stated mathematically as:

$$P_y = \frac{\mu_b(T)\sqrt{(2\pi)}}{\gamma} \tag{2}$$

μ_b is the plastic dynamic viscosity, $\pi = e_{ij}$ denotes the component product of the deformation rate with itself e_{ij} represent the deformation rate, also π_c stands for the critical value according to the Casson fluid model.The Casson liquid motion where $\pi > \pi_c$, can be defined as follows:

$$\mu_0 = \mu_b(T) + \frac{P_y}{\sqrt{2\pi}} \tag{3}$$

When (2) is substituted in (3), it will happen that kinematic viscosity will be influenced by μ_b representing the plastic dynamic viscosity. Additionally the density ρ and Casson term γ are yield to:

$$\mu_0 = \frac{\mu_b(T)}{\rho}\left(1 + \frac{1}{\gamma}\right) \tag{4}$$

In pursuit of accuracy, the investigation delves into the boundary layer approximation based on the presumed validity of the Boussinesq approximation. Subsequently, the following governing equations are formulated.
Equation of continuity:

$$\frac{\partial u}{\partial x} + \frac{\partial v}{\partial y} = 0 \tag{5}$$

Equation of mommentum:

$$u\frac{\partial u}{\partial x} + v\frac{\partial u}{\partial y} = \nu\left(1 + \frac{1}{\gamma}\right)\frac{\partial^2 u}{\partial y^2} - \left(1 + \frac{1}{\gamma}\right)\frac{v}{K_o}u - \frac{\sigma B_0^2}{\rho}u + g\beta_t(T - T_\infty) + g\beta_c(C - C_\infty) + g\beta_n(N - N_\infty) \tag{6}$$

Energy equation:

$$u\frac{\partial T}{\partial x} + v\frac{\partial T}{\partial y} = \frac{\mathrm{k}}{\rho c_p}\left[\frac{\partial^2 T}{\partial y^2}\right] + \frac{\mathrm{k}}{\rho c_p}\left(1 + \frac{1}{\gamma}\right) \times \left[\left(\frac{\partial u}{\partial y}\right)^2 + \left(\frac{\partial v}{\partial y}\right)^2\right] - \frac{1}{\rho c_p} + \left[\frac{\partial}{\partial y}q_r\right] + \frac{\mathrm{Q}_o}{\rho c_p}(T - T_\infty) \tag{7}$$

where $q_r = \frac{16\sigma T^3}{3k}\left[\frac{\partial^2 T}{\partial y^2}\right]$

Species continuity equation (concentration)

$$u\frac{\partial C}{\partial x} + v\frac{\partial C}{\partial y} = D_m\frac{\partial^2 C}{\partial y^2} - k_r(C - C_\infty) \tag{8}$$

Gyrotactic equation

$$u\frac{\partial N}{\partial x} + v\frac{\partial N}{\partial y} = D_n\frac{\partial^2 N}{\partial y^2} - \frac{bW_c}{\Delta C}\left(\frac{\partial N}{\partial y}\frac{\partial C}{\partial y} + \frac{\partial^2 C}{\partial y^2}\right) \tag{9}$$

With respect to the boundary conditions:

$$u = U_w(x)\ \ , v = -v_w(x)\ , T = T_w = T_\infty + b_x\ \ , C = C_w = C_\infty + C_x, N = N_w = N_\infty + p_x\ , \tag{10}$$

$$at\quad y = 0, u \longrightarrow 0,\ v \longrightarrow 0\ , T \longrightarrow T_\infty, C \longrightarrow C_\infty\, N \longrightarrow N_\infty\quad , as\quad y \longrightarrow \infty \tag{11}$$

3.1 Similarity transformation

The stream functions is defined as $\boldsymbol{\psi(x, y)}$ $\boldsymbol{u}$ and $\boldsymbol{v}$ denotes the relations $\boldsymbol{u = \frac{\partial \psi}{\partial y}}$ also $\boldsymbol{v = -\frac{\partial \psi}{\partial x}}$. where it is defined of $\boldsymbol{u}$ and $\boldsymbol{v}$, and the set of similarity ios defined as follows. The

symbol $\boldsymbol{\eta}$ stands for similarity variable, $\boldsymbol{\psi}$ is for dimensionless stream function, $\boldsymbol{\theta(\eta)}$ for temperature and $\boldsymbol{\phi(\eta)}$ for concentration. Their equations are below as:

$$\eta = \left(\frac{U}{\nu}\right)^{\frac{1}{2}} y \quad , \psi = (\nu U x)^{\frac{1}{2}} f(\eta),\ T - T_\infty = (T_w - T_\infty)\theta(\eta),\ C - C_\infty = (C_w - C_\infty)\phi(\eta), N - N_\infty = (N_w - N_\infty)\chi(\eta), u = axf'^{(\eta)}, v = -\sqrt{\nu a}\, f(\eta), \tag{12}$$

where, T_∞ represent ambient temperature and T_w represent temperature at the wall, respectively. C_w denote the concentration at the wall and C_∞ denotes ambient concentration, then N_w and N_∞denote ambient gyrostatic organism and the wall and respectively.

Using the above similarity variables on the flow equation 5 to equation 9 subject to equation 10 we have the following differntial equations

Employing the similarity variables established previously, and applying them to equations 5 through 9 subject to equation 10, yields the following set of differential equations.

$$\left(1 + \frac{1}{\gamma}\right) f''' = (f')^2 - g f'' - \frac{1}{2}\eta f' f'' + \left(M^2 f' + k\left(1 + \frac{1}{\gamma}\right)\right) f' - G_r\theta - G_c\phi \tag{13}$$

13

$$\theta''(1 + Rd) = Ec[\left(f'^{)^2} + \frac{1}{2}\eta^2 f'' - \eta f' f'' + (g')^2\right] + p_r\left[\frac{1}{2}\eta f'\theta' + \theta' g\right] + p_r Q\theta \tag{14}$$

$$\phi'' = Sc\left[kc\phi - \frac{1}{2}\eta\phi' - g\phi'\right] \tag{15}$$

$$\varphi'' = Lbf\varphi' - Pe\varphi'\phi' - Pe\phi''\varphi - Pe\beta_k\phi'' \tag{16}$$

subject to

$$f' = 1, g = s, \theta' = -1, \varphi = 1, as\ \eta = 0$$
$$f = 0, f' \to 0, g \to 0, \varphi \to 0, \theta = 0. as\ \eta = \infty \tag{17}$$

where K is permeability parameter, Pr is Prandtl number, S suction/injection parameter, M^2 magnetic parameter, and Sc Schmidt number. Gr Grashof number for temperature, GC number for concentration, Ec is Eckert number, Rd radiation parameter, Q is internal heat generation/absorption parameter, KC a chemical reaction, Pe is peclet number, Lb is lewis number and β is the constant.

4 Numerical solution of problem

Various numerical approaches employed in many investigations on Casson fluid dynamics, as documented by Verma and Mondal [11], encompass Rung-Kutta 4, Shooting Methods, Keller Box Method, and Spectral Method. Additionally, Goud et al., [12] investigated the Casson fluid phenomenon utilizing the finite element method. In the present study, the Spectral Relaxation method (SRM) is utilized in Matlab to address the numerical aspects of the problem and to visualize the results graphically.

This method involves employing the Chebyshev pseudo-spectral technique for discretizing the linearized equations. The linear term is assessed at the present iteration as $r + 1$, whereas the nonlinear terms are assessed at the preceding iteration, indicated as r.

The basic steps of the spectral approach are:

- Firstly, Gauss-Seidel methods are applied to decouple and linearize the nonlinear equations;

- Next step involves discretizing the linearized equations;
- Employ the Chebyshev pseudo-spectral approach for iteratively solving the discretized equations.

5 Discussion of the results

The complete numerical results of this particular problem as described in this chapter. All of the programmes were written in MATLAB R2012a. The findings were generated using the scaling parameter L = 8, and it was discovered that increasing the value of L does not significantly impact the outcome. The number of collocation point used in generating the results was Nx = 120.

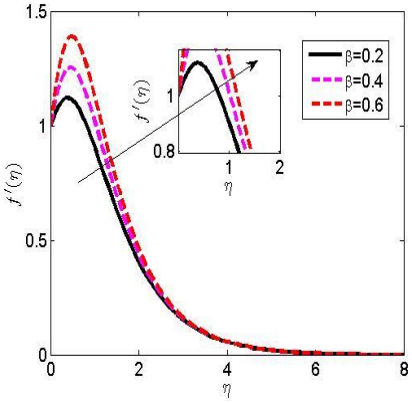

Fig. 1. Effect of Casson parameter on velocity profile.

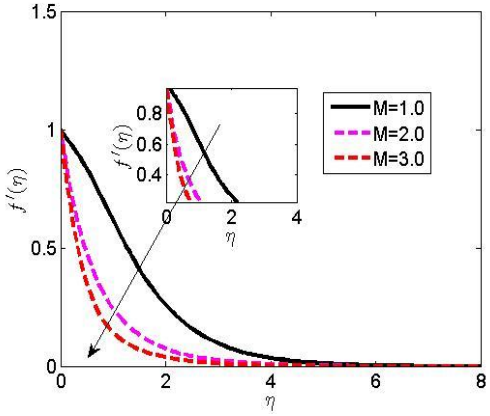

Fig. 2. Effect of magnetic parameter on velocity profile.

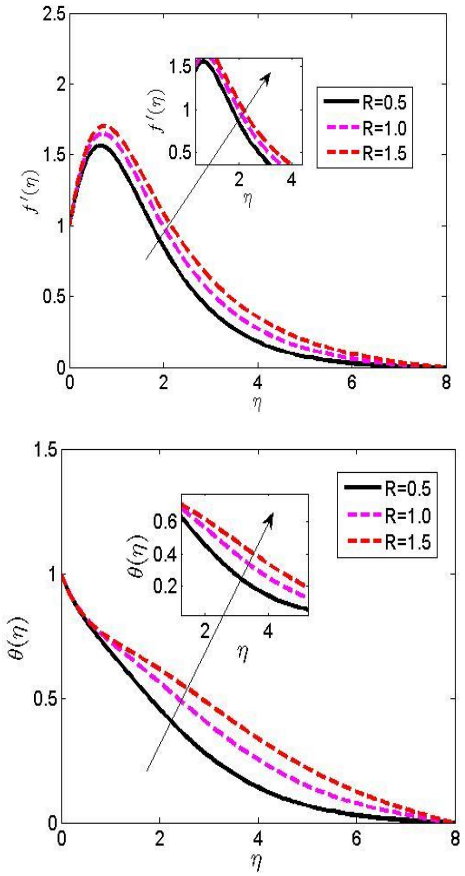

Fig. 3. Effect of thermal radiation parameter on velocity and temperature profiles.

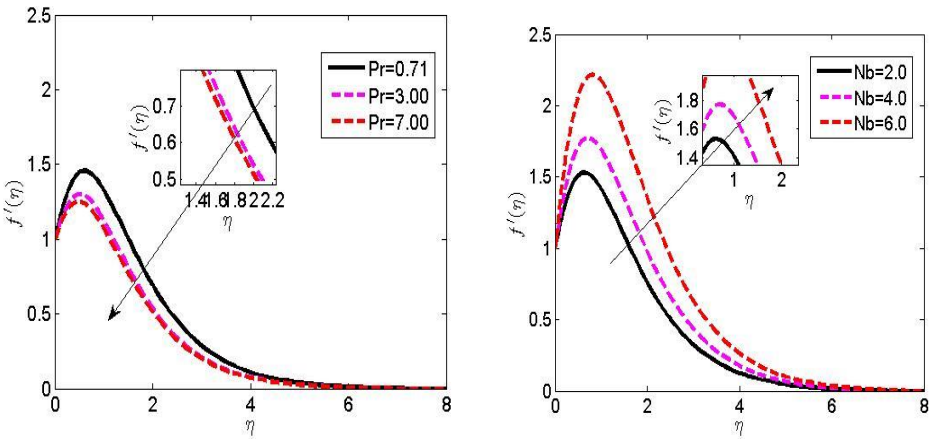

Fig. 4. Effect of Prandtl number on velocity and temperature profiles profiles.

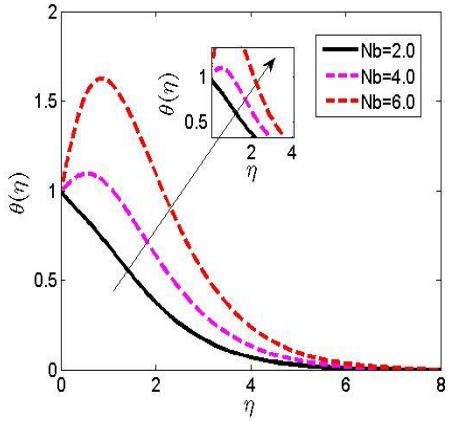

Fig. 5. Effect of Brownian motion parameter on velocity and temperature.

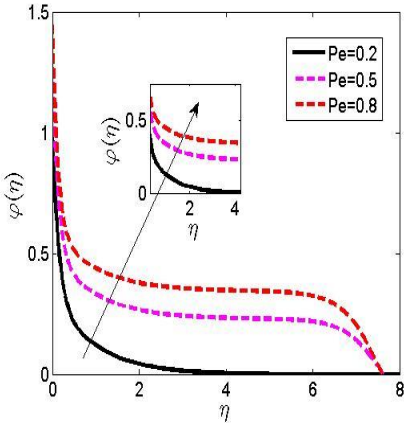

Fig. 6. Effect of Peclet number on velocity and motile density profiles.

Figure 1 illustrates the influence of the Casson parameter (β) on velocity profile, revealing a famous improvement in velocity profile with the improvement of the Casson term. In this study, a blood-based Casson fluid is considered, demonstrating steady flow in the vessels for β values of 0.2, 0.4, and 0.6. As β approaches infinity, indicating a transition to a Newtonian fluid, the flow ceases. Physically, an increase in β signifies an increase in the yield-exhibiting fluid within the boundary layer, leading to an increase in plastic viscosity and the depth of the hydrodynamic boundary layer. Figure 2 showcases the influence of the magnetic parameter (M) on velocity profile, where a decrease in M (1, 2, and 3) results in a corresponding decrease in velocity contour. The perpendicular imposition of the magnetic parameter generates Lorentz force, which generally opposes the flow of electrically conducting fluids. Figure 3 represents the effect of the thermal radiation parameter (R) on velocity and temperature contours, demonstrating a considerable increase in both velocity and temperature profiles with an increase in R. This growing in R leads to an rise in thermal and hydrodynamic boundary layer thicknesses, indicating a significant alteration in the flow regime within the boundary layer due to thermal energy. Figure 4 displays the impact of the Prandtl number (Pr) on velocity and temperature contours, elucidating the mutual relationship between thermal conductivity and kinematic viscosity. An increase in Pr extremely reduces velocity and temperature profiles, signifying greater heat diffusion at higher Pr values. Figure 5 depicts the significance of the Brownian motion parameter on

velocity and temperature contours, indicating that an increase in Nb enhances both velocity and temperature contours. This growth in Nb results in thickening of hydrodynamic and thermal boundary layers. Figure 6 illustrates the influence of the Peclet number (Pe) on velocity and motile density contours, showing higher velocity and motile density profiles with an increase in Pe. This enhancement in Pe leads to an observable increase in the viscosity of the motile density boundary layer, facilitating the distribution of motile microorganisms within the boundary layer. In this subsection, the impact of escalating the magnetic field is investigated across various study configurations. Specifically, the influence of the magnetic field on the primary velocity profile is examined for both Prescribed Surface Temperature (PST) and Prescribed Heat Flux (PHF) cases. It is observed that the primary velocity profile exhibits a gradual decline with increasing magnetic field intensity. Despite the presence of a substantial Lorentz force generated, which serves as a resisting force within the fluid motion at the boundary layer, the primary velocity diminishes in a remarkably smooth manner.

Finally, as the Casson fluid parameter increases under constant miscellaneous parameters, we observe a decrease in the thickness of boundary layers. Concurrently, an increase in the magnetic field leads to accelerated motion along respective paths, accompanied by a decrease in concentration profile. Additionally, heightened permeability tends to expand the boundary layers of the Casson fluid. Conversely, an increase in the Grashof number causes a reduction in the thickness of thermal and concentration layers.

6 Conclusion

In this study, we investigated the influence of viscous dissipation, magnetic field, and thermal radiation on the systematic flow of Casson fluid with gyrotactic microorganisms. Through mathematical modeling and numerical simulations, we aimed to understand the complex dynamics of this fluid system. By employing the spectral relaxation method (SRM) in MATLAB, we were able to numerically solve the governing equations and obtain graphical results for the problem at hand. The SRM approach, utilizing the Chebyshev pseudo-spectral method for discretization, allowed us to accurately capture the behavior of the Casson fluid under various conditions.

Our results revealed significant effects of viscous dissipation, magnetic field, and thermal radiation on the fluid temperature, velocity, and boundary layers. The viscous dissipation parameter (Ec) was found to enhance fluid temperature and velocity, while the magnetic parameter contributed to the generation of Lorenz force, influencing the fluid flow within the boundary layer. Additionally, the presence of nanoparticles had a notable impact on gyrotactic microorganisms. The numerical findings were obtained with careful consideration of parameters such as the scaling parameter and the number of collocation points. It was observed that variations in these parameters did not significantly alter the outcomes, indicating the robustness of our numerical approach. Overall, our study provides valuable insights into the behavior of Casson fluid with gyrotactic microorganisms under the influence of viscous dissipation, magnetic field, and thermal radiation. These findings contribute to the broader understanding of fluid dynamics and have potential applications in various fields, including engineering and biomedicine.

References

1. M.A. Aiyashi, S.M. Abo-Dahab, M.D. Albalwi, Sci. Rep., **13**(1), 22529 (2023)
2. A. Hassan, A. Hussain, M. Arshad, S. Gouadria, J. Awrejcewicz, A.M. Galal, F.M. Alharbi, S. Eswaramoorthi, Front. Phys., **10**, 920372 (2002)
3. R. Kodi, O. Mopuri, S. Sree, V Konduru, Heat Transfe, **51**(1), 377-94 (2022)
4. A.M. Obalalu, J. Egypt. Math. Soc., **30**(1), 6 (2022)
5. M. Qasim, S. Noreen, Eur. Phys. J. Plus, **129**, 1-8 (2014)
6. A. Usman, S.S. Abas, N.A. Jaafar, M.H. Muhammand, M. Mamat, J. Adv. Res. Fluid Mech. Therm. Sci., **105**(2), 31-50 (2023)
7. M. Malik, M. Mamat, S.S. Abas, I.M. Sulaiman, F. Sukono, Eng. Lett., **28**(3), 704-14 (2020)
8. M.H. Muhammad, S.S. Abas, N.A. Jaafar, A. Usman, M. Mamat, J. Adv. Res. Fluid Mech. Therm. Sci., **106**(1), 23-38 (2023)
9. A.S. Idowu, B.O. Falodun, Math. Comput. Simul., **177**, 358-84 (2020)
10. A.G. Fredrickson, Principles and applications of rheology, (1964)
11. V.K. Verma, S. Mondal, Partial Differ. Equ. Appl. Math., **3**,100034 (2021)
12. B.S. Goud, P.P. Kumar, B.S. Malga, Partial Differ. Equ. Appl. Math., **2**, 100015 (2020)